Supplementary Data

Materials and methods

Plasmids and shRNAs

All transfection constructs were derived from vector pAdRSV-Sp. Expression constructs for SENP1, SENP3 and SENP7 were generated by PCR amplification of the corresponding ORFs from P19 cells-derived cDNA, and subsequent insertion in the pAdRSV-Sp vector with an N-terminal Flag tag. Expression constructs for HIF1Am, SUMO1, SUMO2, UBC9, and PIAS1-4 have been previously described.[1, 2] Expression vectors for small hairpin RNA molecules (shRNA) were based on vector pSuper (OligoEngine, Seattle, WA, USA). Control shRNA (5'-CCATCAAGACTCATAGATG-3') and target sequence for *Senp7* (5'-TCAGACTCATTGCCTTCGA-3') were previously described.[3] Other target sequences for shRNA constructs were: *Senp1*, 5'-GGAAAGAGTTTGACACCAA-3'; *Senp3*, 5'-GGAAGAGTCTGGTACTACA-3'. Targeting of human *SENP7* was performed with the TriFECTa DsiRNA Kit (IDT, Coralville, IA, USA), using a *luciferase siRNA* (target sequence: 5'-CGUACGCGGAAUACUUCGA-3') as a control.

Cell culture and transfection

Murine P19 cells, directly purchased from ATCC (LGC Standards, Barcelona, Spain) as authenticated, were routinely cultured in Dulbecco's modified Eagle's medium (DMEM) (Sigma-Aldrich, St. Louis, MO, USA) supplemented with 10% fetal bovine serum (FBS) (Sigma-Aldrich). Previous reports indicate that these cells are suitable for sumoylation studies.[3-5] HCT116 cells were cultured in McCoy's 5A medium supplemented with 2 mM glutamine and 10% FBS. Absence of mycoplasms was verified in all cells. OGD treatment was achieved by culturing the cells at the indicated times in DMEM without glucose in HEPA Class 100 incubators (Thermo Fisher Scientific, Waltham, MA, USA) with 1% oxygen, after over-night equilibration of the medium. For harmful OGD, cells were exposed to a 20 h-period of OGD. $CoCl_2$ was used at 150 µM. $NaAsO_2$ was used at 100 µM. DMOG (Sigma-Aldrich) was used at 100 µM. Heat shock was performed in HEPA incubators at 42º C. Transfections of plasmids and shRNA vectors were performed with Lipofectamine 2000 (Invitrogen, Life Technologies, Paisley, UK) for 24 and 72 h, respectively. Transfection of siRNAs was performed with Lipofectamine RNAiMAX (Invitrogen) for 72 h.

Cytotoxicity measurement

Citotoxicity was measured either through lactate dehydrogenase (LDH) activity determination as through determination of Anexin V/propidium iodide (PI) labeling/incorporation by flow cytometry. For this purpose, Pierce™ LDH Cytotoxicity Assay Kit (Thermo Fisher Scientific) and FITC Annexin V Apoptosis Detection Kit with PI (immunostep, Salamanca, Spain) kits were used, respectively, according to manufacturer instructions. Samples for determination of Anexin V/PI incorporation were analyzed in a BD FACSCalibur flow cytometer (BD Biosciences, San Jose, CA, USA).

Western blot

For Western blot analysis, proteins were separated in SDS gels and transferred to PVDF membranes (GE Healthcare, Buckinghamshire, UK) for antibody hybridization. Signal was revealed with the chemiluminescence ECL system (Bio-Rad) reactive and recorded in a ChemidDoc XRS apparatus (Bio-Rad). Antibodies were as follows: mouse anti-Flag M2 (1:2000; Sigma-Aldrich), rat anti- HA (1:2000; Roche, Mannheim, Germany), mouse anti-α-tubulin (1:10,000; Sigma), rabbit anti-Senp7 (1:1000, abcam, Cambridge, UK, ab187126), rabbit anti-HIF1A (1:1000, Cayman chemical, Ann Arbor, MI, USA, 10006421), and horseradish peroxidase-conjugated goat anti- mouse IgG, anti-rat IgG and anti-rabbit IgG (1:10,000; Sigma-Aldrich).

Expression analysis

For the analysis of gene expression, total RNA was extracted using the NZYTech Total RNA isolation kit (NZYTech, Lisbon, Portugal), which was retro-transcribed with the iScript cDNA Synthesis kit (Bio-Rad). Quantitative PCR (qPCR) was performed with Power SYBR Green (Applied Biosystems, Carlsbad, CA, USA) in the 7500 Fast Real-Time PCR System (Applied Biosystems). *RpLp0* and *GAPDH* housekeeping genes were used as the reference for the analysis of relative expression in P19 and HCT116 cells, respectively, being data normalized according to.[6] Primers were: *RpLp0*, forward 5'-CCAGGCTTTGGGCATCAC-3', reverse, 5'-CTCGCTGGCTCCCACCTT-3'; *GAPDH*, forward 5'-GAGTCAACGGATTTGGTCGT-3', reverse 5'-AATGAAGGGGTCATTGATGG-3'. Other primers are described in.[3]

Database and statistical analyses

Two-tailed Student's t test was applied for statistical analysis of two groups (comparison with control), and one-way ANOVA ($p < 0.05$) followed by multiple comparison Tukey's post-test was applied for statistical analysis of more than two groups. *$p < 0.05$, **$p < 0.01$, ***$p < 0.001$. Normal distribution and similar variances were assumed. For expression analysis, three independent experiments were analyzed in triplicate. For cytotoxicity measurements, three independent experiments were performed. Represented values are means ± s.d. Results were double-blind assessed (group allocation and outcomes). RNA-seq expression (RSEM normalized), copy number variation and clinical data were obtained from The Cancer Genome Atlas (http://cancergenome.nih.gov) using Pan-Cancer cohort.[7] Survival plots and the log-rank test were performed using GraphPad Prism version 5.0. For tumor description, the Tumor–Node– Metastasis (TNM) staging system (https://cancerstaging.org) was used, whereby T followed by a number (1–4) describes the extent of the tumor (with T4 being the largest). No subdivisions of stages were used. Significance of differences were computed using Prism 5 (GraphPad) and either Student's *t* test or Chi-square test, with confidence interval of 95%. Association of SENP7 expression levels with survival outcomes in different cohorts shown in Supplemental Table 1 were collected from the PrognoScan database (dna00.bio.kyutech.ac.jp/PrognoScan/).[8] COX regression analysis[9] parameters (hazard ratios, HR*;* confidence intervals, CI; and COX *p*-values), were obtained directly from PrognoScan. Only studies with COX *p*-values ≤ 0.01 were considered as significant. Data about perturbation effects on HCT116 cells by *SENP7* interference were obtained from RNAi (Achilles+DRIVE+Marcotte, DEMETER2) dataset at (https://depmap.org/portal/).[10]

Supplementary Figures

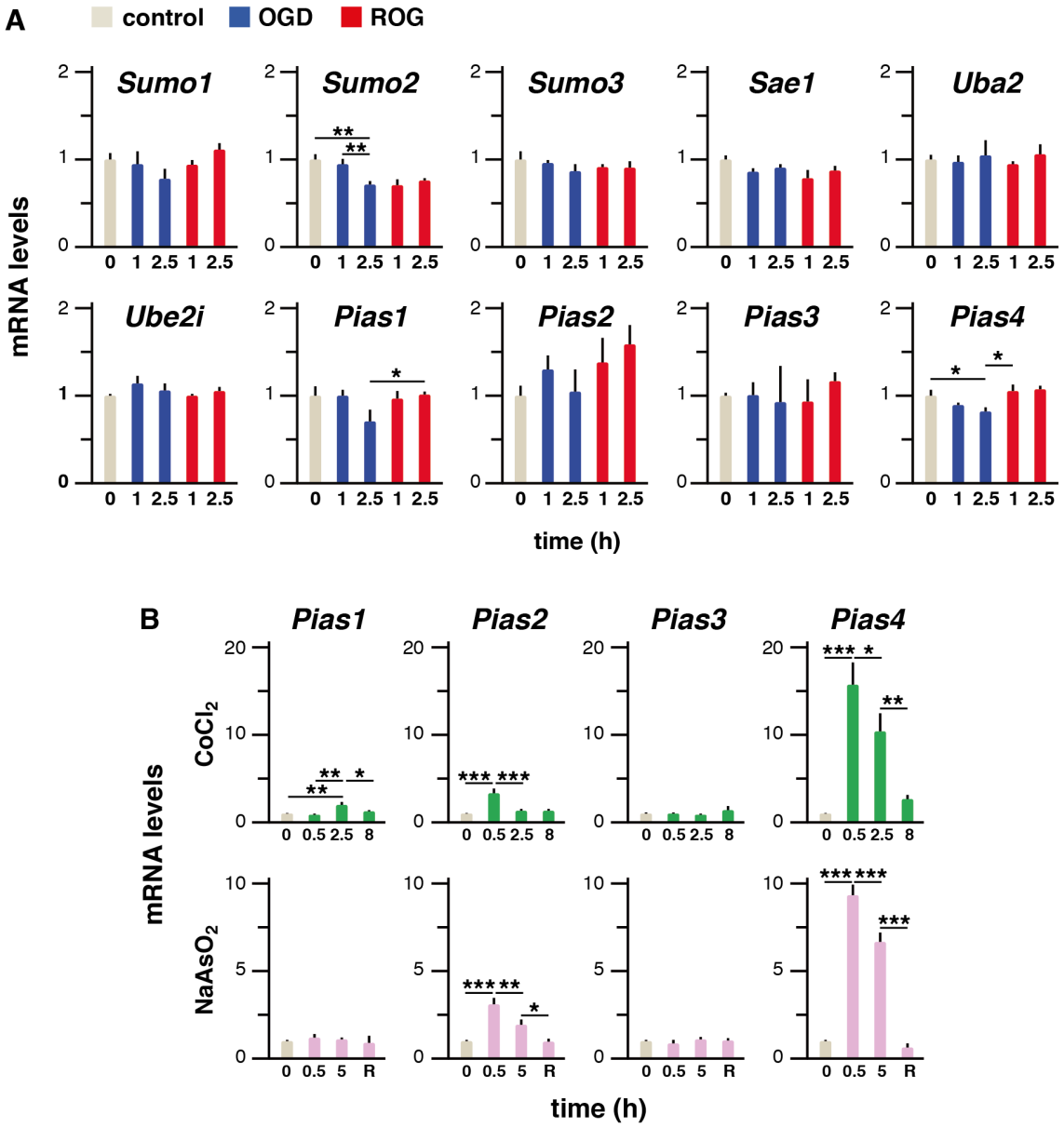

Figure S1. Expression of components of the sumoylation pathway are regulated by OGD/ROG conditions. **(A)** Relative mRNA levels of the indicated genes, as determined by quantitative PCR (qPCR), in control P19 cells (0) or cells subjected to OGD and ROG (after 2.5 h of OGD) for the indicated times. **(B)** Relative mRNA levels of *Pias* genes, as determined by qPCR, in response to treatment with the hypoxia mimetic cobalt chloride[11] or the cytotoxic agent arsenite[12] for the indicated times. In the case of arsenite, levels were also determined after 24 h of normal growth conditions restoration (R) in cells treated with arsenite for 0.5 h. **(A, B)** Levels were normalized to the levels at 0 h. Values are means ± s.d. of three independent experiments analyzed in triplicate. Statistical significance of changes in gene expression was analyzed by one-way ANOVA ($p < 0.05$) followed by the Tukey's post-test: *$p < 0.05$, **$p < 0.01$, ***$p < 0.001$.

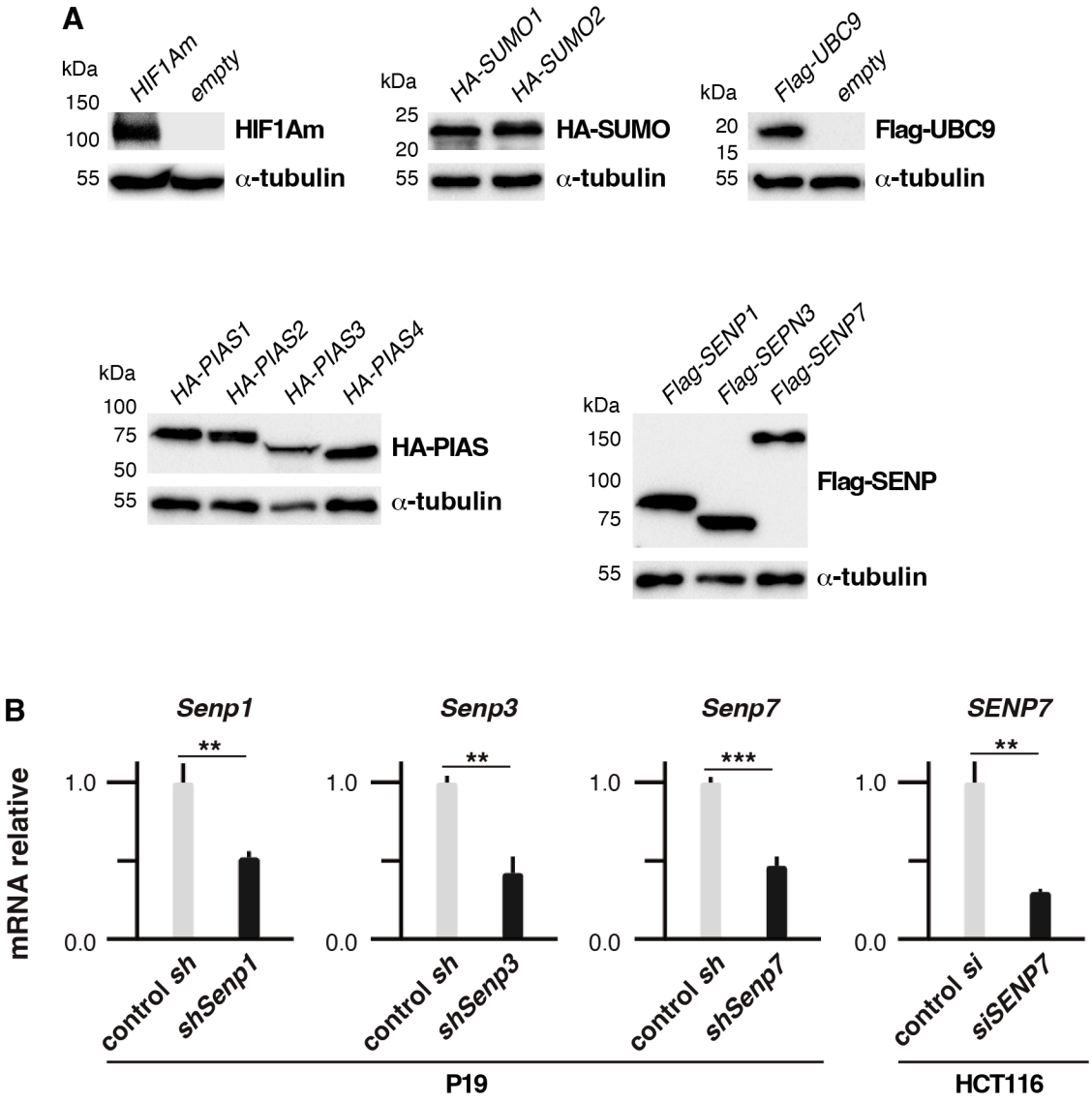

Figure S2. Expression in P19 cells of the different proteins analyzed in this work and effect of *shRNA* and *siRNA* molecules. **(A)** Protein levels of the indicated HA- or Flag-tagged constructs or mutant HIF1A[2] (HIF1Am) were analyzed by Western blot with HA, Flag or HIF1A antibodies, respectively, after transfection of the corresponding expression constructs in P19 cells. Control determinations in cells transfected with empty vector are included in some cases. 30 µg of total protein were loaded per lane. α-tubulin levels were determined as a loading control. **(B)** mRNA levels for *Senp1*, *3* and *7* genes in P19 cells and of *SENP7* gene in HCT116 cells were determined by qPCR after expression of a control *shRNA* (sh) molecule or sh molecules against the corresponding mRNAs in P19 cells, or after transfection of a control *siRNA* (*si*) or a *siRNA* against *SENP7* in HCT116 cells. Values are means ± s.d. of three independent experiments analyzed in triplicate. Statistical significance of differences was analyzed by the Student's t-test: **p* < 0.05, ***p* < 0.01, ****p* < 0.001.

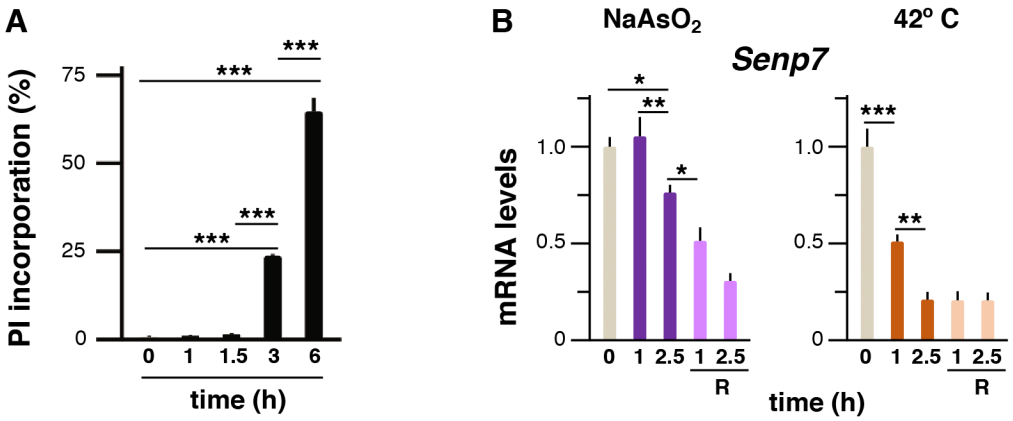

Figure S3. Effects of arsenite and heat shock on *Senp7* mRNA levels. **(A)** Propidium iodide (PI) incorporation, as determined by flow cytometry, was analyzed in cells treated with arsenite for the indicated times. Values are means ± s.d. of three independent determinations. **(B)** mRNA levels were determined by qPCR in cells treated with arsenite or subjected to heat shock at 42º C, for the indicated times. Samples were also taken at the indicated times after restoring (R) normal growth conditions following 2.5 h of treatment. Levels were normalized to the levels at 0 h. Values are means ± s.d. of three independent experiments analyzed in triplicate. **(A, B)** Statistical significance of differences was analyzed by one-way ANOVA ($p < 0.05$) followed by the Tukey's post-test: *$p < 0.05$, **$p < 0.01$, ***$p < 0.001$.

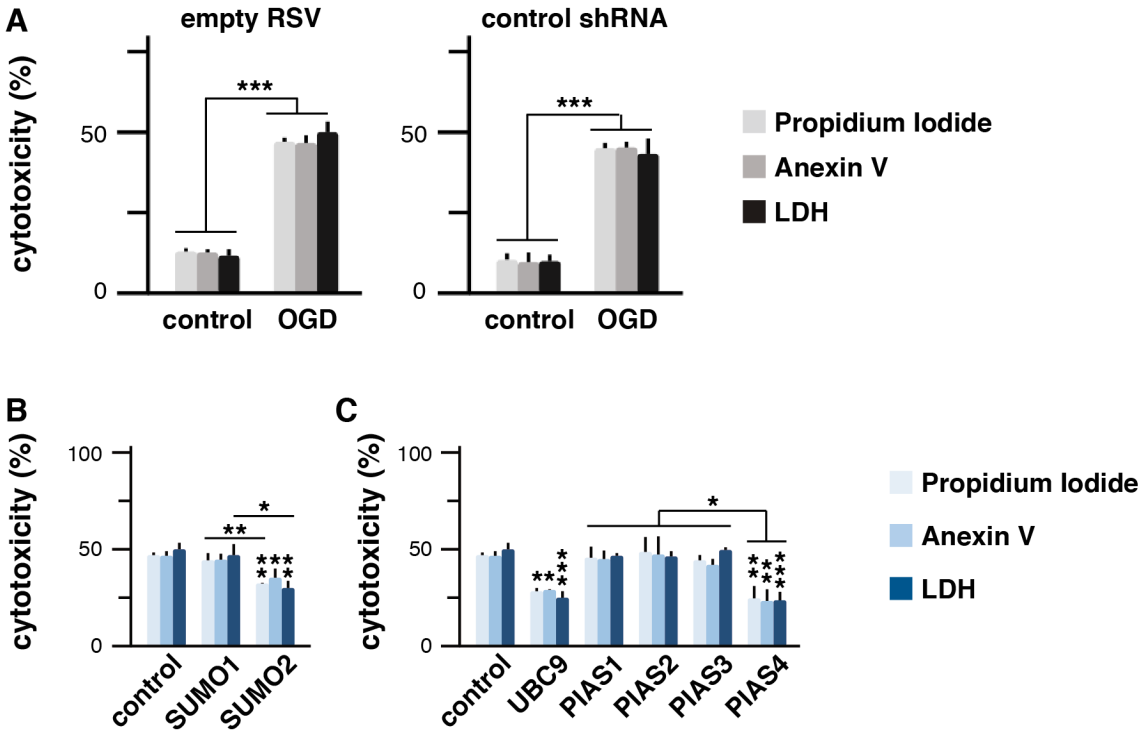

Figure S4. Effect of expression of SUMO pathway components on cytotoxicity after harmful OGD. **(A)** The percentage of cytotoxicity was determined in P19 cells subjected or not (control) to harmful OGD by propidium iodide or Anexin V labeling, or by measurement of LDH activity, after transfection of the empty vector for protein expression (RSV) or a vector expressing a control shRNA. Statistical significance of differences in cytotoxicity was analyzed by the Student's t-test. **(B, C)** The percentage of cytotoxicity was determined in P19 cells subjected to harmful OGD after transfection of expression constructs for SUMO1 and 2 (B); or expression constructs for UBC9 and PIAS1-4 (C). Statistical significance of differences in cytotoxicity was analyzed by one-way ANOVA ($p < 0.05$) followed by the Tukey's post-test. **(A-C)** Values are means ± s.d. of three independent determinations. Differences in relation to the corresponding control are indicated on top of each bar. Differences between groups of samples are indicated with lines: *$p < 0.05$, **$p < 0.01$, ***$p < 0.001$.

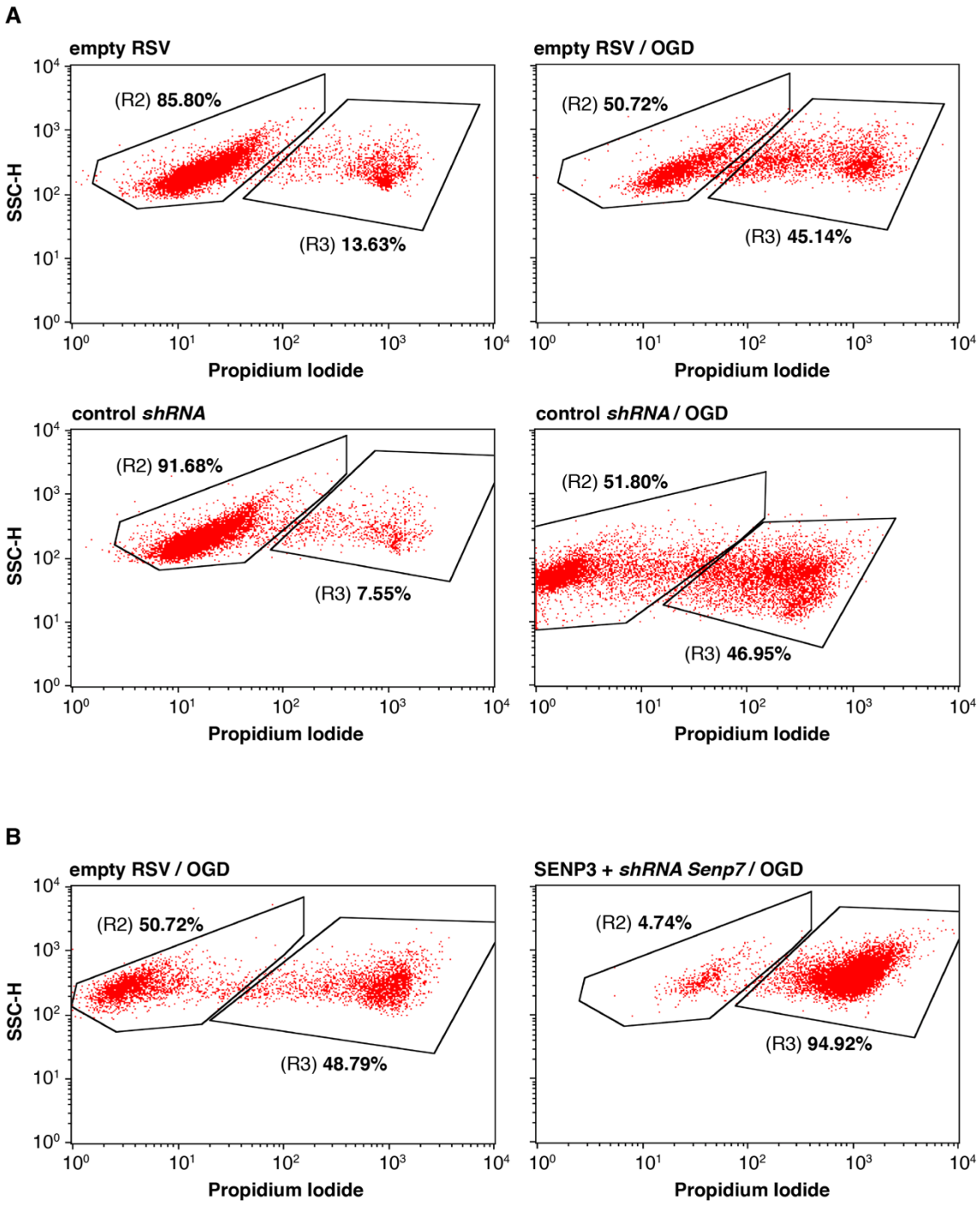

Figure S5. Propidium iodide incorporation under OGD conditions. The percentage of cytotoxicity was determined in P19 cells subjected (OGD) or not to harmful OGD by propidium iodide (PI) incorporation, after **(A)** transfection of the empty vector for protein expression (RSV) or a vector expressing a control shRNA, and **(B)** transfection of empty RSV or an expression construct for SENP3 together with an expression construct for a *shRNA* against *Senp7*. The percentage of cells incorporating (R3) or not incorporating (R2) PI is indicated.

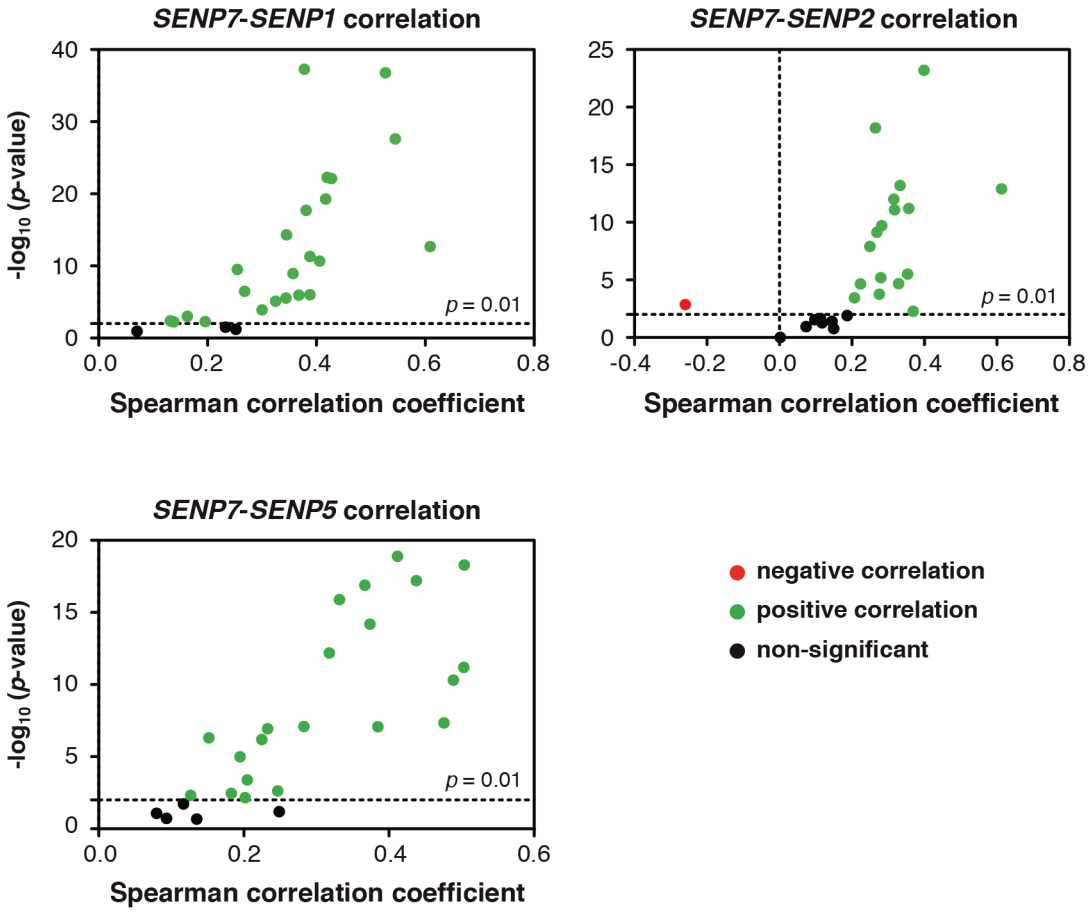

Figure S6. Correlation of mRNA levels of *SENP7* with those of *SENP1*, *SENP2* and *SENP5* in cancer cells. Volcano plots showing Spearman correlation coefficient versus –$\log_{10}$ (*p*-value) for the correlation between mRNA levels of *SENP7* and *SENP1*, *SENP2* or *SENP5* in different types of tumors.

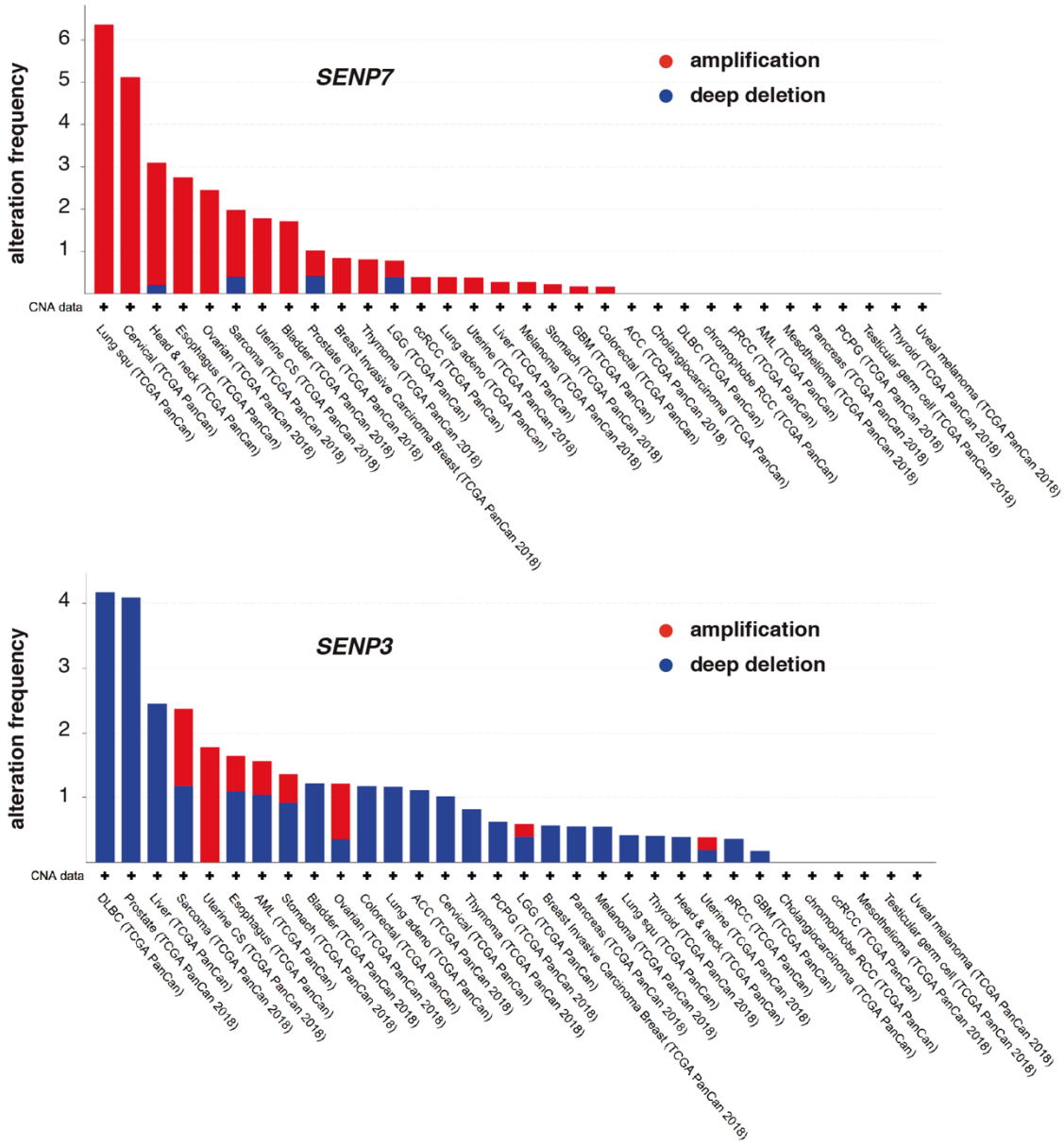

Figure S7. Genomic alterations of *SENP7* and *SENP3* regions in cancer cells. Frequency of alteration in genomic regions containing *SENP7* and *SENP3* genes are represented in relation to amplifications or deep deletions for the indicated tumors. The PanCancer cohort (n=10967 samples) from TCGA was used through cBioportal.

Supplementary Table

Table S1. Cox regression analysis of the correlation between *SENP7* tumor mRNA levels and patient survival in different colon adenocarcinoma studies using COX regression analysis.[9]

Dataset	Endpoint	HR	CI	COX *p*-value
GSE17537	Overall Survival	31.21	[3.71 - 262.15]	0.0015
	Disease Free Survival	4.94	[1.72 - 14.17]	0.003
	Disease Specific Survival	4.24	[1.51 - 11.90]	0.006
GSE17536	Disease Specific Survival	2.31	[1.26 - 4.21]	0.006
	Overall Survival	1.99	[1.17 - 3.40]	0.011
	Disease Free Survival	2.72	[1.16 - 6.39]	0.021
GSE14333	Disease Free Survival	2.29	[1.24 - 4.23]	0.008
GSE12945	Disease Free Survival	7411.3	[1.36 -40248.3]	0.042

Data were collected from PrognoScan.[8] GEO dataset reference is provided. COX regression analysis parameters (hazard ratios, HR; confidence intervals, CI; and COX *p-values*) are shown. A positive HR value indicates that the analyzed risk increases when the level of gene expression increases, and thus the prognosis is worse. Different survival endpoints (overall survival, disease-free survival, and disease specific survival) are shown. Only studies with COX *p-values* ≤ 0.01 were considered as significant.

Additional Discussion

Deregulation of SUMO modification is tightly linked to cancer (reviewed in[13]), being involved in cancer initiation, progression, metastasis and chemoresistance. Besides notable involvement of SENP7 in promoting cell survival, we have also observed that PIAS4 overexpression leads to enhanced survival under deleterious OGD conditions. In relation to this, it has been reported that PIAS4 is upregulated in hypoxia, mediating sumoylation of the tumor suppressor protein VHL, which results in abolition of its inhibitory function on tumor growth, migration and clonogenicity.[14] More interestingly, an important role has been assigned to SUMO protease dysfunction in disrupting SUMO homeostasis to facilitate cancer development and progression.[15] Solid evidence strongly links SENP7 with several types of cancer.[16, 17] In contrast, an antitumor function has been proposed for SENP3. It has been suggested that SENP3 is a redox sensor,[18, 19] which accumulates and is activated in the presence of reactive oxygen species to facilitate STING-mediated antitumor function in dendritic cells.[20] Thus, the absence of SENP3 drives tumor progression. Notably, SUMO proteases have been proposed as potential targets for cancer therapy.[21] Therefore, our results suggest that the careful design of drugs for selective inhibition of SENP7 might be of great value for treating cancer, in particular colon cancer.

Acknowledgements

We thank P. García-Gutiérrez for critical reading of the manuscript, and M. Dana and M.J. Quintero for assistance at cell culture and flow cytometry core facilities, respectively. We also thank A. López-Rivas for providing HCT116 cells. The results shown here are in part based upon data generated by the TCGA Research Network: https://www.cancer.gov/tcga.

References

1. Garcia-Gutierrez P, Juarez-Vicente F, Gallardo-Chamizo F, Charnay P, Garcia-Dominguez M. The transcription factor Krox20 is an E3 ligase that sumoylates its Nab coregulators. *EMBO Rep*. 2011;12(10): 1018-23.
2. Masson N, Willam C, Maxwell PH, Pugh CW, Ratcliffe PJ. Independent function of two destruction domains in hypoxia-inducible factor-alpha chains activated by prolyl hydroxylation. *EMBO J*. 2001;20(18): 5197-206.
3. Juarez-Vicente F, Luna-Pelaez N, Garcia-Dominguez M. The Sumo protease Senp7 is required for proper neuronal differentiation. *Biochim Biophys Acta*. 2016;1863(7 Pt A): 1490-8.
4. Ceballos-Chavez M, Rivero S, Garcia-Gutierrez P, et al. Control of neuronal differentiation by sumoylation of BRAF35, a subunit of the LSD1-CoREST histone demethylase complex. *Proc Natl Acad Sci USA*. 2012;109(21): 8085-90.
5. Correa-Vazquez JF, Juarez-Vicente F, Garcia-Gutierrez P, Barysch SV, Melchior F, Garcia-Dominguez M. The Sumo proteome of proliferating and neuronal-differentiating cells reveals Utf1 among key Sumo targets involved in neurogenesis. *Cell Death Dis*. 2021;12(4): 305.
6. Pfaffl MW. A new mathematical model for relative quantification in real-time RT-PCR. *Nucleic Acids Res*. 2001;29(9): e45.
7. Consortium ITP-CAoWG. Pan-cancer analysis of whole genomes. *Nature*. 2020;578(7793): 82-93.
8. Mizuno H, Kitada K, Nakai K, Sarai A. PrognoScan: a new database for meta-analysis of the prognostic value of genes. *BMC Med Genomics*. 2009;2: 18.

9. Cox DR. Regression models and life tables. *J Roy Statist Soc B.* 1972;34: 187-202.
10. Tsherniak A, Vazquez F, Montgomery PG, et al. Defining a Cancer Dependency Map. *Cell*. 2017;170(3): 564-76 e16.
11. Hirsila M, Koivunen P, Xu L, Seeley T, Kivirikko KI, Myllyharju J. Effect of desferrioxamine and metals on the hydroxylases in the oxygen sensing pathway. *FASEB J*. 2005;19(10): 1308-10.
12. Hughes MF, Beck BD, Chen Y, Lewis AS, Thomas DJ. Arsenic exposure and toxicology: a historical perspective. *Toxicol Sci*. 2011;123(2): 305-32.
13. Xie M, Yu J, Ge S, Huang J, Fan X. SUMOylation homeostasis in tumorigenesis. *Cancer Lett*. 2020;469: 301-9.
14. Cai Q, Verma SC, Kumar P, Ma M, Robertson ES. Hypoxia inactivates the VHL tumor suppressor through PIASy-mediated SUMO modification. *PLoS One*. 2010;5(3): e9720.
15. Bawa-Khalfe T, Yeh ET. SUMO Losing Balance: SUMO Proteases Disrupt SUMO Homeostasis to Facilitate Cancer Development and Progression. *Genes Cancer*. 2010;1(7): 748-52.
16. Bawa-Khalfe T, Lu LS, Zuo Y, et al. Differential expression of SUMO-specific protease 7 variants regulates epithelial-mesenchymal transition. *Proc Natl Acad Sci USA*. 2012;109(43): 17466-71.
17. Zhu H, Ren S, Bitler BG, et al. SPOP E3 Ubiquitin Ligase Adaptor Promotes Cellular Senescence by Degrading the SENP7 deSUMOylase. *Cell Rep*. 2015;13(6): 1183-93.
18. Huang C, Han Y, Wang Y, et al. SENP3 is responsible for HIF-1 transactivation under mild oxidative stress via p300 de-SUMOylation. *EMBO J*. 2009;28(18): 2748-62.
19. Wang Y, Yang J, Yang K, et al. The biphasic redox sensing of SENP3 accounts for the HIF-1 transcriptional activity shift by oxidative stress. *Acta Pharmacol Sin*. 2012;33(7): 953-63.
20. Hu Z, Teng XL, Zhang T, et al. SENP3 senses oxidative stress to facilitate STING-dependent dendritic cell antitumor function. *Mol Cell*. 2021;81(5): 940-52 e5.
21. Tokarz P, Wozniak K. SENP Proteases as Potential Targets for Cancer Therapy. *Cancers (Basel)*. 2021;13(9): 2059.